

Cationic Host–Guest Polymerization of *N*-Vinylcarbazole and Vinyl Ethers in MCM-41, MCM-48, and Nanoporous Glasses

Stefan Spange,^{*[a]} Annett Gräser,^[a] Andreas Huwe,^[b] Friedrich Kremer,^[b] Carsten Tintemann,^[c] and Peter Behrens^[c]

Abstract: The synthesis of poly(vinyl ether)s or polyvinylcarbazole under the conditions of constricted geometry can be achieved by means of cationic host–guest polymerisation of the corresponding monomers in the pores of MCM-41 (pore diameter 3.6 nm), MCM-48 (pore diameter 2.4 nm) and in nanoporous glasses (Gelsil[®] with a pore diameter of 5 nm) with bis(4-methoxyphenyl)methyl chloride (BMCC) or triphenylmethyl chloride as the internal surface initiator. The reaction products are new polymer/MCM-41, polymer/MCM-48 etc., host–

guest hybrid materials. The molecular mass of the enclosed polymer and the degree of loading of the host compounds can be adjusted within certain limits. The molecular dynamics were investigated by using broad-band dielectric spectroscopy. Under the conditions of

Keywords: organic–inorganic hybrid composites • polymerization • vinylcarbazole • vinyl ether • zeolites

constricted geometry, molecular fluctuation is observed as well as a secondary β -relaxation, which is hardly affected (in comparison with the free melt) and which corresponds to the relaxation between structural substates (dynamic glass transition). This process is several orders of magnitude faster in its relaxation rate than in the free melt and thus follows a confinement effect. This is already well known in lower molecular weight systems with constricted geometry.

Introduction

The study of flexible polymers under the conditions of constricted geometry, such as that found in cavities or nanopores of inorganic or organic solid materials (see Figure 1), is an experimental challenge. From theoretical studies carried out by de Gennes it can be expected that, for example, the glass transition point of enclosed flexible polymer chains is significantly affected by the pore geometry of the host.^[1, 2] As the thickness of the polymer layer decreases, as a consequence of the space available, the glass transition temperature should decrease. Various experimental procedures are available for the preparation of individual polymer chains within solid materials. Individual polymer chains can be enclosed by sol-

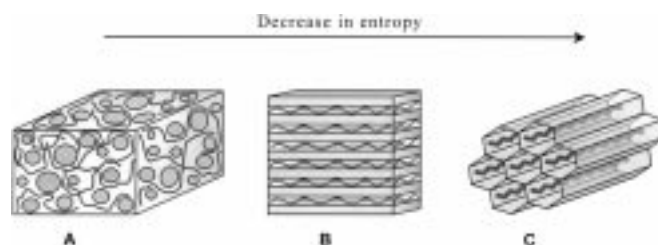


Figure 1. Morphologies of polymer/inorganic-oxide hybrid materials. A) sol-gel polymer/silica gel hybrid; B) polymer in the layered silicate; C) individual polymer chains in MCM-41.

gel processes in a hybrid material, deposited in two dimensions in layered silicates or adsorbed in nanopores of solid porous materials. Figure 1 shows possible morphologies of deposited polymer structures.

In recent years there have been many publications on polymer/sol-(xero)gel hybrid materials and on the deposition of synthetic polymers in layered silicates.^[3–14] The threading of linear flexible chains in highly ordered pore systems of HY zeolites or MCM-41 (method 1) is experimentally very difficult, as direct threading appears to be relatively unsuccessful because of the associated loss of entropy (see Figure 2). A further option involves the synthesis of the polymer directly in the pore system of a mesoporous silicate or other host (method 2).

[a] Prof. Dr. S. Spange, Dr. A. Gräser
Polymer Chemistry, Department of Chemistry
Faculty of Natural Science, Chemnitz University of Technology
09107 Chemnitz (Germany)
Fax: (+49)371-531-1642
E-mail: stefan.spange@chemie.tu-chemnitz.de

[b] A. Huwe, Prof. Dr. F. Kremer
Faculty of Physics and Geological Sciences
University of Leipzig
Linnéstrasse 5, 04103 Leipzig (Germany)

[c] C. Tintemann, Prof. Dr. P. Behrens
Institute for Inorganic Chemistry, University of Hannover
Callinstrasse 9, 30167 Hannover (Germany)

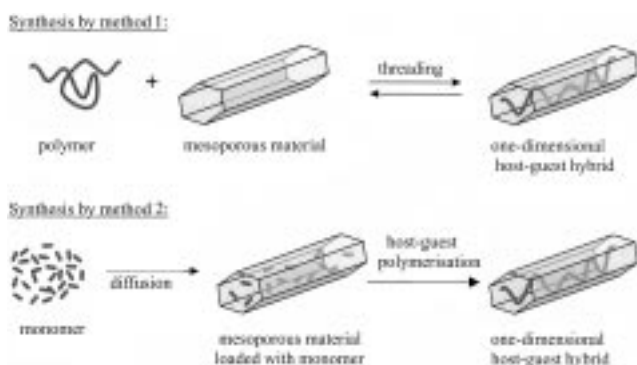


Figure 2. Syntheses of one-dimensional polymer/oxide hybrids.

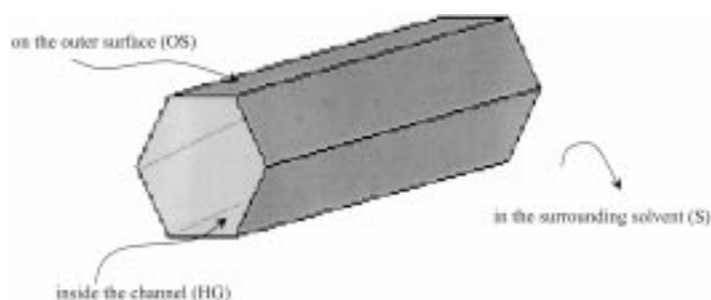
Various methods have been developed for host–guest polymerisation. The pioneering work of Bein should be mentioned in particular.^[15–21] He successfully studied the electropolymerisation of pyrrole in HY zeolites and the radical polymerisation of methacrylates in MCM-41. In these processes the initiation of the polymerisation occurs by chance on or within the solid material, as the initiator used is added in dissolved form. If the initiator is immobilised by covalent bonding to the inner surface of a mesoporous silicate or an aluminosilicate, a method used successfully with transition metal complexes for ethylene polymerisation, polyethylene fibres can be synthesised directly inside the mesopores of, for example, MCM-41.^[22–27] Mesoporous silicates internally grafted with polyethylene are thus formed.

One problem with all host–guest polymerisations is that the inner surface chemistry of the host compounds must interfere as little as possible, if at all, with the mechanism of the polymerisation reaction, for example, by inducing transfer and degradation reactions. In the cationic polymerisation of vinyl ethers in nanopores of moderately acidic HY zeolites, acid-induced reactions of the poly(vinyl ether) in the pore system of the zeolite occur, resulting in ether cleavage and conjugated polymer sequences.^[28]

Results and Discussion

We now present an extension of the concept of guest synthesis of individual polymer chains in the pores of MCM-41 and MCM-48 hosts, and mesoporous glasses and report for the first time on the determination of the glass transition temperatures of enclosed, flexible polymer chains by using dielectric spectroscopy. We used cationic surface polymerisation as the synthesis method.^[29–32] We chose substituted vinyl ethers [(2,3-dihydrofurans (DHF), ethyl vinyl ether (EVE), 2-chloroethyl vinyl ether (CIEVE), and isobutyl vinyl ether (IBVE)] as the monomers (M) so that the size of the monomer molecule and the glass transition temperature of the (bulk) polymer formed could be adjusted by varying the substituents and the reactivity of the double bond. We also used *N*-vinylcarbazole (NVC). Our knowledge and experience of the mechanism of cationic surface polymerisation allowed us to adjust the reaction conditions in such a way that the polymerisation occurs preferentially in the silicate channels. Equation (1)

gives an expression for the rate of total monomer consumption, taking into consideration the reaction steps of the cationic propagation reactions in the channels (host–guest, HG), those on the outer surface of the MCM-41 (OS) and in the surrounding solution (S) (see also Scheme 1). If there is



Scheme 1. Possible courses of cationic polymerisation on porous materials.

exclusive cationic host–guest polymerisation the second and third terms in Equation (1) amount to zero.

$$-\frac{d[M]}{dt} = k_{\text{pHG}}[R^+]_{\text{HG}}[M]_{\text{HG}} + k_{\text{pOS}}[R^+]_{\text{OS}}[M]_{\text{OS}} + k_{\text{pS}}[R^+]_{\text{S}}[M]_{\text{S}} \quad (1)$$

This can best be achieved experimentally by adjusting the concentration of the carbenium ion in the surrounding solution $[R^+]_{\text{S}}$ or on the outer surface $[R^+]_{\text{OS}}$ in such a way that the contributions from second and third terms to the overall turnover of the monomer is minimalised. Arylmethyl halides $[X-CR^1R^2R^3]$ are used as cationically inactive initiators for this so-called host–guest polymerisation. They are essentially inactive in solution, but are activated specifically on the inner surface of porous silicate materials, for example.^[33] A particularly useful initiator for cationic host–guest polymerisations is $(4-CH_3OC_6H_4)_2CHCl$. When it is adsorbed on the surface of the silicate, heterolytic bond cleavage occurs at the central carbon–halogen bond. The ion formed, $(4-CH_3OC_6H_4)_2CH^+$, can be detected directly by UV-visible transmission spectroscopy in MCM-41, measured in the suspension by using light-conducting optics (Figure 3).^[29]

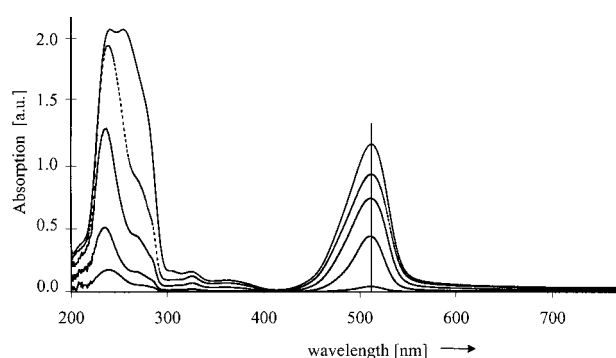


Figure 3. Formation of $(4-CH_3OC_6H_4)_2CH^+$ as a function of time during the adsorption of $(4-CH_3OC_6H_4)_2CHCl$ in MCM-41 measured using UV-visible transmission spectroscopy in dichloromethane at room temperature (22 °C). Peaks centered at about 250 nm and 500 nm: top to bottom, 140, 45, 27, 4 s.

The transmission technique allows the carbenium ion fraction to be determined within the mesopores, because as a result of the high transparency of MCM-41 suspended in CH_2Cl_2 , these UV-visible absorptions can be measured accurately. The influence of light scattering on the position of UV-visible absorption can be neglected.

Figure 3 shows the increase in the UV-visible absorption of the carbenium ions with time during the adsorption of $(4\text{-CH}_3\text{OC}_6\text{H}_4)_2\text{CHCl}$ in MCM-41. The formation of $(4\text{-CH}_3\text{OC}_6\text{H}_4)_2\text{CH}^+$ can be clearly recognised from the characteristic UV-visible absorption at $\lambda = 511 \text{ nm}$.^[33] The largest fraction of $(4\text{-CH}_3\text{OC}_6\text{H}_4)_2\text{CH}^+$ in terms of quantity is fixed in the channels of the MCM-41, because on nonporous carriers, such as Aerosil® 300, no time-dependence is observed, but instead complete adsorption occurs within seconds.^[29] Furthermore it reacts very rapidly with vinyl ethers or *N*-vinylcarbazole, so that the conditions for rapid initiation and thus molecular mass control of the polymer fraction formed are given (see Figure 4).^[34]

The deviation of the experimental curve from the theoretical one (see legend to Figure 4) can be attributed to the fact that not all the $(4\text{-CH}_3\text{OC}_6\text{H}_4)_2\text{CHCl}$ (R-Cl) is available and, therefore, is not all consumed during the initiation. This means that the actual concentration of $[\text{R}^+]$ is lower than the quantity of RCl used (see Experimental Section).

The initiation of the host-guest polymerisation is achieved by rapid addition of the diarylmethyl carbenium ion to the double bond of the vinyl monomer.^[29, 32] After addition of the monomer to the $(4\text{-CH}_3\text{OC}_6\text{H}_4)_2\text{CH}^+/\text{MCM-41}$ composite about three minutes of diffusion time are required until the initiator (BMCC) is consumed (determined by direct UV-visible measurement of the decrease in the absorption of the $(4\text{-CH}_3\text{OC}_6\text{H}_4)_2\text{CH}^+$ at $\lambda = 511 \text{ nm}$ in the suspension). However, initiation can also be

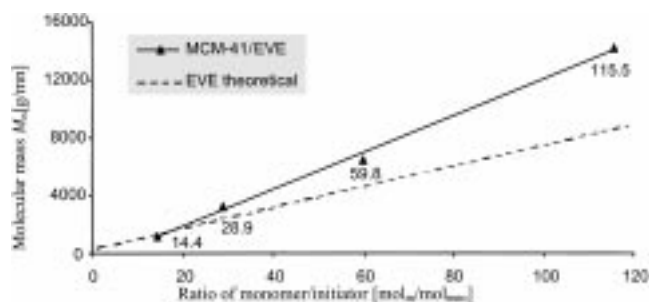
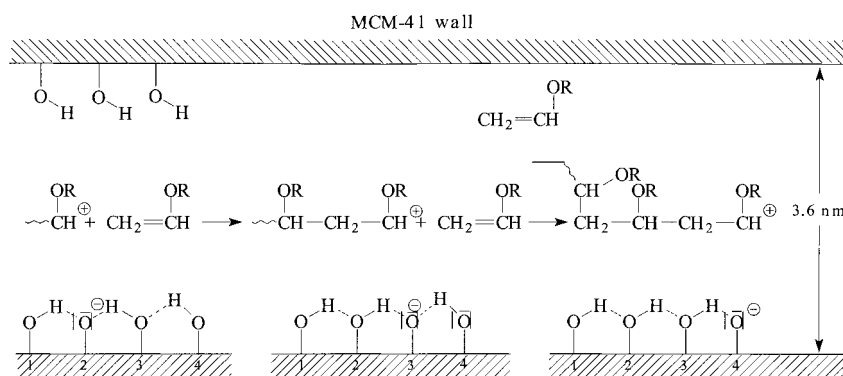


Figure 4. Molecular mass of extracted PEVE as a function of the ratio of the quantity of monomer to the quantity of initiator BMCC with exact details of the M/I ratio in the diagram. The theoretical curve (dashed) was calculated as follows: $M_n = M_0[\text{M}]/[\text{I}] + M_{\text{BMCC}}$. M_0 : molecular mass of EVE; $[\text{M}]$: quantity of EVE; $[\text{I}]$: quantity of initiator bis-(4-methoxyphenyl)methyl chloride (MeO); M_{BMCC} : molecular mass of BMCC.

achieved by very low concentrations of particularly acidic protons on the inner surface of the MCM-41 skeleton.^[35] The propagation reaction proceeds through addition of further monomer molecules to the active chain, whereby the chain itself does not move within the channel, but monomer diffusion towards the chain determines the propagation rate, since the counterion can migrate as a result of very rapid proton exchange between the silanol groups on the inner surface area of MCM-41,^[30, 31] in other words, the exchange of silanol protons on the inner MCM-41 surface proceeds more rapidly than the propagation of the polymer. We presume the overall entropy loss, which has to be overcome during direct threading, is distributed over the individual steps of the propagation reaction and is compensated for by the reaction energy liberated in each addition step. Scheme 2 shows the mechanistic principles of the cationically induced host-guest polymerisation.

In this way many vinyl monomers that undergo cationic polymerisation can be converted into the corresponding polymer in the cavities of inorganic materials. Table 1 shows the results of selected vinyl ether and NVC polymerisations in MCM-41.



Scheme 2. Suggestion for the course of cationic propagation reaction of vinyl ethers in an MCM-41 channel. The silanol group density is not correct.

Table 1. Overview of the mass (m) of the monomer used and the quantity (n) of monomer which actually remains in the channel as polymer. For a better comparison the mass of polymer formed per gram MCM-41 is also given.

System	$m_{\text{Monomer}}/m_{\text{MCM-41}}$ [mg _M per g _C]	$m_{\text{Polymer}}/m_{\text{MCM-41}}$ [mg _P per g _C]	$n_{\text{Polymer}}/m_{\text{MCM-41}}$ ^[a] [mmol _P per g _C]
MCM-41/DHF	5948	494	7.04
MCM-41/EVE	7292	411	5.69
MCM-41/CIEVE	8006	427	4.00
MCM-41/CHVE	9117	465	3.68
MCM-41/IBVE	7765	380	3.52
MCM-41/NVC	5597	333	2.76
MCM-41/styrene	10022	100	0.96
MCM-41 ^[b]		500	5.94
PA-Cu-MCM-41 ^[c]		160	1.72
PMMA-MCM-41 ^[d]		590	5.89

[a] n_{Polymer} refers to the quantity of monomer polymerised in the channel which remains there as polymer. [b] The loading of an MCM-41/silicate hybrid (pore diameter 3.0 nm) with cyclohexane is given as 0.5 g_{cyclohexane} per g_{MCM-41} at $p/p_0 = 0.4$, which corresponds to 5.94 mmol_{cyclohexane} per g_{MCM-41} according to ref. [36]. [c] Polymerisation of aniline in Cu-MCM-41 (pore diameter 3 nm) according to ref. [18]. [d] Polymerisation of methyl methacrylate (MMA) in MCM-41 (pore diameter 3 nm) according to ref. [21].

The solid hybrid materials obtained by cationic host–guest polymerisation contain up to 30 wt% carbon as determined by quantitative elemental analysis.^[38a] As the comparison with the results of other host–guest polymerisations from the literature shows, the data in Table 1 lie within the expected range. Part of the polymer fraction cannot be removed from the MCM-41 by simple extraction with an organic solvent. This indicates strong binding of the polymer to the inner surface of the solid. Residual monomer or unreacted initiator is extracted completely. Solid-state NMR investigations (¹³C and ²⁹Si) have so far not given any unambiguous indication as to whether the poly(vinyl ether) formed is actually covalently bonded to the inner MCM-41 wall by an Si–O–CHR¹OR bond. Since acetals or ketals react readily with silanol groups forming Si–O–CHR¹OR bonds,^[37] this option is very likely, especially as acetaldehyde diethyl acetal reacts smoothly with MCM-41 with the loss of ethanol.^[38] However, it is very difficult to differentiate between the ¹³C NMR signal of the C atom of the Si–O–C bond and that of the poly(vinyl ether).^[38] Furthermore in the poly(vinyl ether) ($M_n = 4000 \text{ g mol}^{-1}$)/MCM-41 hybrid there are approximately 40 ether bonds for one possible Si–O–C bond, so that the resolution of the corresponding signal is particularly difficult.

To characterise the molecular mass distribution and the structures of the enclosed polymers more precisely it was necessary to dissolve the PVE/MCM-41 hybrid in KOH.

We established that the number average molecular weight (M_n) of the guest poly(vinyl ether) fraction rarely exceeds 4000 g mol^{-1} in the case of IBVE or 2-chloroethyl vinyl ether, independent of the starting monomer concentration or the temperature used. Theoretical considerations with regard to the effective channel length in MCM-41 and the contour size of the whole guest-polymer fraction show that the ratio of $r_{\text{cont}}/l_{\text{MCM-41}}$ (r_{cont} = contour length, l = channel length), in the case of smaller monomers, such as DHF or EVE, is significantly larger than for NVC or CHVE.

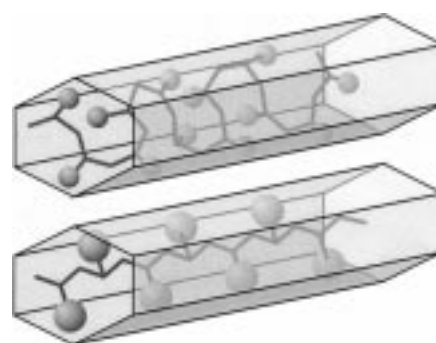
Since the contour length is a theoretical parameter—the actual chain length of the enclosed polymer in MCM-41 is significantly smaller—a maximum of 4–5 chains should be deposited together (estimation) (Table 2 and Scheme 3).

The pore volume of MCM-41 hybrids decreases continuously with increasing polymer loading in all the samples

Table 2. Comparison of the calculated contour length sum of the polymers with respect to the channels available in MCM-41.

System	$m_{\text{Polymer}}/m_{\text{MCM-41}}$	$\Sigma r_{\text{cont}}^{[a]} [\times 10^{10} \text{ m}]$	$\Sigma r_{\text{cont}}/l_{\text{MCM-41}}^{[b]}$
MCM-41/DHF	0.493	110	16.3
MCM-41/EVE	0.358	76	11.5
MCM-41/EVE	0.196	40	6.3
MCM-41/CIEVE	0.487	67	10.6
MCM-41/IBVE	0.333	51	7.7
MCM-41/CHVE	0.412	51	7.6
MCM-41/NVC	0.532	40	6.4
MCM-41/styrene	0.100	14	2.2

[a] r = contour length. The contour length is the maximum length of a polymer in the fully elongated conformation. The calculation of the contour length is based on the total mass of the polymer. [b] l = channel length. Uniform cylinder-shaped pores are assumed for the calculation of the channel length of the MCM-41. The length $l_{\text{MCM-41}} = 6.66 \times 10^{10} \text{ m}$ per $\text{g}_{\text{MCM-41}}$ was calculated from the BET surface area and the determined pore radius.



Scheme 3. Schematic comparison between polymers with differently sized substituents in MCM-41. The upper part shows a spiral polymer with small side groups in the channel (e.g., PEVE). A polymer with significantly larger groups (e.g., PNVC) should be almost entirely stretched out in the channel, as shown in the lower part.

investigated. The pore radius distribution in the hybrid material becomes correspondingly wider, as can be seen, for example, in the case of MCM-41/PCHVE hybrids (Figure 5). It can be recognised that in the hybrid material pores

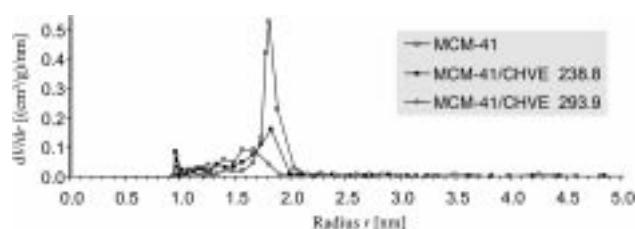


Figure 5. The change in the volume of adsorbed nitrogen with respect to the pore radius gives an indication of the pore radius distribution of the starting material MCM-41 and of two samples loaded with polymer PCHVE.

with a smaller radius ($r = 1.1$ to 1.8 nm) exist alongside with the pores of unloaded MCM-41 ($r = 1.82 \text{ nm}$).

For the dielectric investigations we chose poly(ethyl vinyl ether) (PEVE)/ and poly(isobutyl vinyl ether) (PIBVE)/MCM-41 hybrid materials, as in both cases the corresponding organic polymer fractions have a glass transition temperature of about -40°C in the pure bulk and, therefore, can be investigated particularly easily within a temperature range of approximately -150°C to 100°C .

Figure 6 shows two dielectric loss spectra of the poly(isobutyl vinyl ether) (PIBVE)/MCM-41 hybrid at different temperatures. Two relaxation processes can be recognised. The rapid β -relaxation process is attributed to movement of the side groups. The dynamic glass transition (α -relaxation) corresponds to the relaxation of the main chain between structural substates.

Figure 7 shows the logarithmic relaxation rate as a function of the reciprocal temperature for PIBVE in the free melt and in MCM-41. The relaxation rate of the local β -relaxation of PIBVE in MCM-41 does not differ from that of the free polymer melt (bulk phase). The dynamic glass transition, on the other hand, is shifted by many orders of magnitude in its frequency position and changes with temperature. While in the free melt the temperature dependence of the relaxation rate follows the (empirical) Vogel–Fulcher–Tammann law (VFT)^[39–41] [$\log 1/\tau = \log 1/\tau_0 - DT_0/(T - T_0)$], Arrhenius-

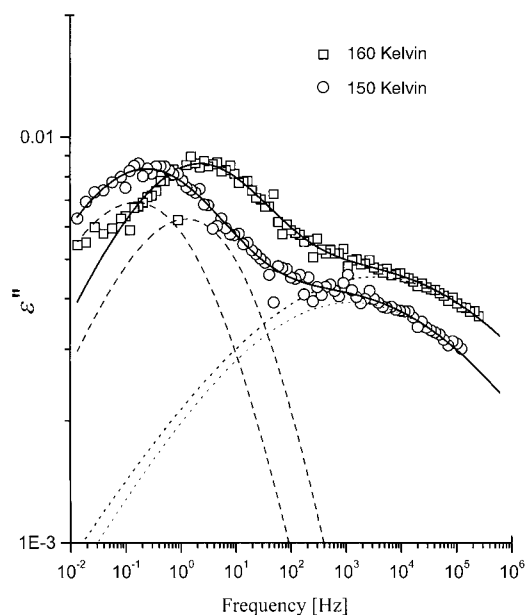


Figure 6. Dielectric loss as a function of the frequency for the hybrid PIBVE/MCM-41 at 150 K (boxes) and 160 K (circles). The lines are an approximation to the relaxation process of model functions according to Havriliak–Negami.^[48] The dashed curve describes the α -relaxation, the dotted curve the β -relaxation and the line represents the sum of both contributions.

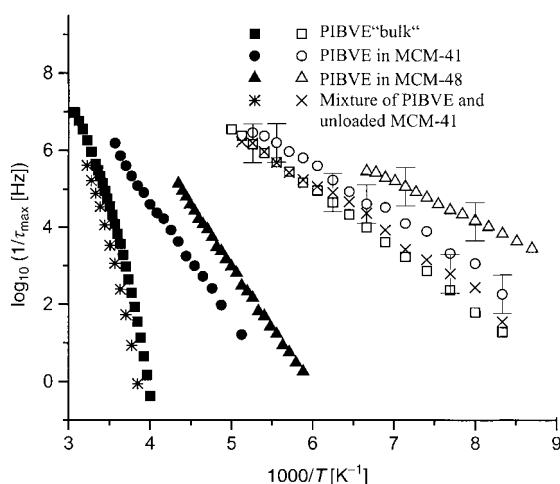


Figure 7. Logarithmic relaxation rate of PIBVE in the free melt (squares), in MCM-41 (circles) and in MCM-48 (triangles) as a function of the reciprocal temperature. The rates for the α -relaxation are shown by closed symbols, the data for β -relaxation by open symbols. Both hybrid materials were tempered at 310 K before measurement. The relaxation rates of the α -relaxation (stars) and the β -relaxation (crosses) are also shown for a mixture of PIBVE and unloaded MCM-41. Where no error bars are shown, these are smaller than the symbols used.

like behaviour is observed for the same molecular process in the constricted geometry of MCM-41 ($\log 1/\tau \propto -E_A/kT$). The VFT Law is characterised by an apparent activation energy that becomes greater as the temperature decreases; the Arrhenius law, on the other hand, implies a temperature-independent activation energy E_A . The calorimetric glass transition corresponds to the temperature at which the relaxation rate is about 0.01 s^{-1} for dynamic measurements. The results of the glass transition temperature determination are shown in Tables 3 and 4.

Table 3. Glass transition temperatures of the polymer fractions determined by DSC.

System	T_g [$^{\circ}\text{C}$]
extractable polymer fraction PNVC $M_n = 34000 \text{ g mol}^{-1}$	197
physical mixture ^[a] PNVC + MCM-41 (carbon content: 29.2 %)	nd ^[b]
hybrid (carbon content: 30.6 %)	nd
extractable polymer fraction PNVC $M_n = 50000 \text{ g mol}^{-1}$	212
extractable polymer fraction PNVC $M_n = 84000 \text{ g mol}^{-1}$	216
extractable polymer fraction PDHF $M_n = 14000 \text{ g mol}^{-1}$	62–69
enclosed polymer fraction PDHF ^[c] $M_n = 4300 \text{ g mol}^{-1}$ in MCM-41 (carbon content: 22.6 %)	52
	nd

[a] The mixtures were prepared by adsorption of the extractable polymer fraction on dried MCM-41 in suspension. [b] nd = not detectable. No endothermic heat absorption could be measured and, therefore, no glass transition temperature. [c] The enclosed hybrid polymer was isolated after dissolving out the silicate part of the hybrid.

Table 4. The glass transition temperatures of the extractable polymer fractions, the polymer fractions enclosed in the hybrid, and polymers physically adsorbed on MCM-41 determined by dielectric spectroscopy.

System	T_g [K]
PCHVE	
PCHVE (polymer)	311
MCM-41/CHVE (hybrid)	no dynamic T_g
PCHVE + MCM-41 (mixture) ^[a]	320
PEVE	
PEVE (polymer)	239
MCM-41/EVE (hybrid)	131
PEVE + MCM-41 (mixture) ^[a]	245
PDHF	
PDHF (polymer)	not detectable, 335 ^[b]
MCM-41/PDHF (hybrid)	128
– after tempering at 310 K	144
PIBVE	
PIBVE (polymer)	244
MCM-41/IBVE ^[c] (hybrid)	135
– after tempering at 310 K	172
– after tempering at 350 K	185
MCM-41/IBVE ^[d] (hybrid)	138
MCM-41/IBVE (hybrid)	139
– after tempering at 350 K	no dynamic T_g
– storage for 14 h in a stream of nitrogen	no dynamic T_g
– storage for 14 h in air	140
PIBVE + MCM-41 (mixture) ^[a]	252
MCM-48/IBVE (hybrid) ^[e]	134
– after tempering at 350 K	166
– absorption of dichloromethane ^[f]	126
– after tempering at 350 K	173
– absorption of cyclohexane ^[f]	143
– after tempering at 350 K	168
– absorption of water ^[f]	123
PIBVE in porous glass Gelsil [®] (hybrid) ^[g]	155

[a] The mixtures were prepared by adsorption of the extractable polymer fraction on dried MCM-41 in suspension. [b] The glass transition temperature of the polymer could be determined by using differential scanning calorimetry and is 335 K (62°C). [c] Hybrid prepared by using the initiator bis-(4-methoxyphenyl)methyl chloride. [d] Hybrid prepared by using the initiator triphenylmethyl chloride. [e] Pore diameter 2.5 nm. [f] Absorption of a particular solvent was achieved by storage of the sample in a desiccator in the corresponding atmosphere for 12 h. [g] Pore diameter 5.0 nm.

The fact that the relaxation rate of the polymer in the hybrids is many orders of magnitude greater than in the free melt can be attributed to the constricting geometry of the channels in porous silicates. If, on the other hand, a polymer melt is mixed with unloaded MCM-41 powder, a slight lowering of the relaxation rate is observed because of surface effects (Figure 7). In the calorimetric glass transition this would be shown by a shift to higher temperatures.

The increase in the relaxation rate of PIBVE in the constricted geometry of the MCM materials is more pronounced when the pore radius is smaller. This is shown by the comparison of PIBVE in MCM-41 (pore diameter 3.6 nm) and MCM-48 (pore diameter 2.4 nm) (see Figure 7). Such a confinement effect has been investigated in detail for low-molecular-weight systems.^[42–44] This effect has its molecular basis in the inherent length scale of the dynamic glass transition, which can increase to values of a few nm with decreasing temperature.^[42, 46–48] The PIBVE polymer chain in the porous channels of the MCM is surrounded by solvent molecules, which facilitate segmental fluctuations. As a result of annealing (at 350 K) a certain fraction of these solvent molecules, which act in some way as a plasticiser, is removed. This leads to a pronounced decrease of the mobility of fluctuating polymer segments (Figure 8). Furthermore, a

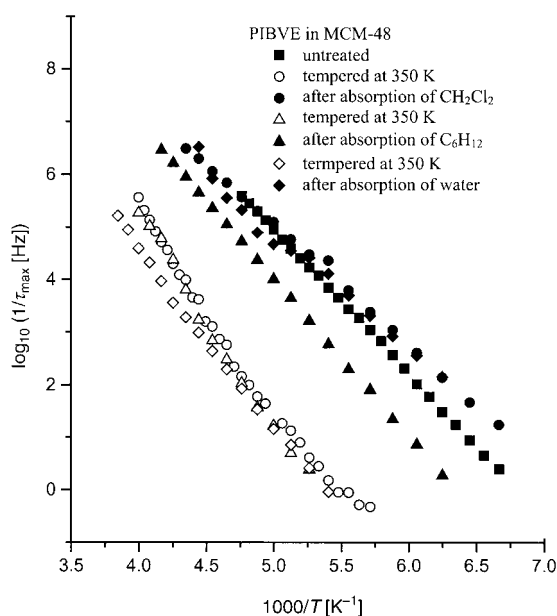


Figure 8. Logarithmic relaxation rate of the α -relaxation of PIBVE in MCM-48 as a function of the reciprocal temperature after tempering (closed symbols) and the absorption of solvents (dichloromethane, cyclohexane and water; open symbols). The sequence of treatment steps corresponds to the sequence of the symbols in the legend.

considerable fraction of the chain will be immobilised. The effect is fully reversible as proven for several solvents (dichloromethane, cyclohexane and water).

Experimental Section

Pretreatment and preparation of the chemicals and M41S materials used: Hexagonal MCM-41 was prepared from KOH (0.33 M, 7.4 mL), tetraethoxysilane (TEOS; 1.64 mL) and dodecyltrimethylammonium bromide (1.16 g). Cubic MCM-48 was obtained from KOH (0.33 M, 7.8 mL),

TEOS (1.22 mL) and tetradecyltrimethylammonium bromide (1.60 g). The reaction mixtures were stirred for 90 min in open vessels and then heated in Teflon-coated stainless steel autoclaves for two days in a circulating air oven at 110 °C. After cooling, the products obtained were filtered and thoroughly washed with hot distilled water. Calcination was carried out at 600 °C for 2 h. The MCM-48 material exhibited clearly resolved peaks typical for polymerisation of that phase up to a diffraction angle of $2\theta \approx 6^\circ$.

The solvents ethanol, hexane, carbon tetrachloride, toluene and dichloromethane, and the monomers EVE, IBVE, CHVE, CIEVE (99 %, Aldrich), MP, styrene and DHF were dried over calcium hydride. All chemicals were distilled before use. NVC was recrystallised from hexane.

In order to achieve complete desorption of the reversibly bound water from the nanoporous carriers, the latter were baked out in a muffle oven at a rate of 1 K min⁻¹ from room temperature to 400 °C. This temperature was then maintained for at least 12 h. The hot carriers were then transferred to Schlenk tubes under argon, cooled in their containers and kept in them until use. Generally they were used immediately after cooling.

General procedure for the polymerisation of EVE, IBVE, CHVE, CIEVE, St, NVC and DHF with initiators on the carriers MCM-41, MCM-48, KG 60 and porous glass: The baked-out support was transferred under argon to a Schlenk tube and then covered immediately with dry dichloromethane (10–20 mL). Renewed water absorption was thus avoided. MCM-41 (ca. 100 mg) or MCM-48 (ca. 100 mg), KG 60 (ca. 500 mg) or 1–2 sheets of porous glass were used. The Schlenk tube was then tempered for 10 min and a weighed quantity of the arylmethyl initiator added (typical quantities: $m_{\text{MeO}} = 100$ mg; $n_{\text{MeO}} = 37$ mmol). Formation of the carbocation on the surface could be observed immediately by the colouration of the support. With bis-(4-methoxyphenyl)methyl chloride an orange-red carbocation with UV-visible absorption at 511 nm was formed immediately, and with triphenylmethyl chloride a yellow carbocation with UV-visible absorptions at 411 nm and 435 nm was formed. After addition of 0.10 to 2.0 mL monomer with stirring, the support tended to become decolourised, although not always completely. The polymerisations were carried out at –25 °C, unless otherwise stated. The reaction was finished after 24 h and the polymer worked up. The support was separated from the solvent and from the soluble extractable polymer by suction filtration on a G4 glass frit. The support was washed with dichloromethane (3 × 15 mL). The combined solvent fractions were washed with aqueous 5% sodium hydrogen carbonate solution (20 mL) to remove acid and dried over sodium sulfate. In the case of PEVE, PIBVE, and PCIEVE the dichloromethane was removed on a rotary evaporator and the remaining polymer was dried in vacuo. The solutions of the polymers PCHVE, PDHF, PSt, and PNVC were concentrated to about 10 mL and the polymers precipitated in ice-cold methanol (150 mL), collected by suction filtration and dried in vacuo.

The polymer obtained (PEVE and PIBVE) was viscous to highly viscous (depending on the molecular mass), sticky and colourless. PCIEVE was obtained in viscous form as a yellow-brown polymer. PCHVE, PDHF, PSt and PNVC were white powders.

The silicate part of the MCM-41 polymer hybrid was readily soluble in aqueous potassium hydroxide. The hybrid (ca. 100 mg) was suspended in 5% potassium hydroxide (30 mL) and covered with hexane (30 mL). The mixture was shaken for about 30 min until the hybrid had completely dissolved. The polymer previously enclosed in the hybrid passed into the organic phase. After phase separation the aqueous phase was then extracted with hexane (2 × 10 mL). The combined organic phases were dried with sodium sulfate, filtered and evaporated. The polymer obtained is completely freed from solvent in vacuo. The poly(vinyl ether)s are resistant to the aqueous potassium hydroxide solution used. An extractable polymer fraction was treated with the solution and worked up as described above. The molecular mass distributions were identical before and after the analogous treatment of the polymer.

Acknowledgements

This work was supported by the DFG within the framework of the programme “Nanoporous Host–Guest Systems”. We also thank the SFB 294 “Molecules Interacting with Interfaces” and the Fonds der Chemischen Industrie.

- [1] K. Dalnoki-Veress, J. A. Forrest, P. G. de Gennes, J. R. Dutcher, *J. Phys. IV* **2000**, *10*, 221–226.
- [2] P. G. de Gennes, *Eur. Phys. J. E* **2000** in press.
- [3] “Hybrid Inorganic–Organic Composites”: *ACS Symp. Ser.*, **1995**, 585, whole issue.
- [4] L. L. Beecroft, C. K. Ober, *Chem. Mater.* **1997**, *9*, 1302–1317.
- [5] H. L. Frisch, J. E. Mark, *Chem. Mater.* **1996**, *8*, 1735–1738.
- [6] J. Wen, G. L. Wilkes, *Chem. Mater.* **1996**, *8*, 1667–1681.
- [7] J. Shi, C. J. Seliskar, *Chem. Mater.* **1997**, *9*, 821–829.
- [8] Y. Ikeda, S. Kohjiya, *Polymer* **1997**, *17*, 4417–4423.
- [9] R. Tamaki, K. Naka, Y. Chujo, *Polym. Bull.* **1997**, *39*, 303–310.
- [10] R. Tamaki, T. Horiguchi, Y. Chujo, *Bull. Chem. Soc. Jpn.* **1998**, *71*, 2749–2756.
- [11] a) J. V. Crivello, Z. Mao, *Chem. Mater.* **1997**, *9*, 1554–1561; b) J. V. Crivello, Z. Mao, *Chem. Mater.* **1997**, *9*, 1562–1569.
- [12] M. Biswas, S. S. Ray, *Polymer* **1998**, *39*, 6423–6428.
- [13] S. S. Ray, M. Biswas, *Mater. Res. Bull.* **1999**, *34*, 1187–1194.
- [14] A. Matsumoto, T. Kitajima, K. Tsutsumi, *Langmuir* **1999**, *15*, 7626–7631.
- [15] J. L. Meinershagen, T. Bein, *J. Am. Chem. Soc.* **1999**, *121*, 448–449.
- [16] C.-G. Wu, T. Bein, *Science* **1994**, *264*, 1757–1759.
- [17] C.-G. Wu, T. Bein, *Chem. Mater.* **1994**, *6*, 1109–1112.
- [18] T. Bein, P. Enzel, *Angew. Chem.* **1989**, *101*, 1737–1738; *Angew. Chem. Int. Ed.* **1989**, *28*, 1692–1694.
- [19] P. Enzel, T. Bein, *J. Phys. Chem.* **1989**, *93*, 6270–6272.
- [20] K. Möller, T. Bein, R. X. Fischer, *Chem. Mater.* **1998**, *10*, 1841–1852.
- [21] K. Möller, T. Bein, *Chem. Mater.* **1998**, *10*, 2950–2963.
- [22] S. M. Ng, S. Ogino, T. Aida, K. A. Koyano, T. Tatsumi, *Macromol. Rapid. Commun.* **1997**, *18*, 991–996.
- [23] S. M. Ng, S. Ogino, T. Aida, K. A. Koyano, T. Tatsumi, *Macromol. Rapid. Commun.* **1997**, *18*, 991–996.
- [24] P. Lehmus, B. Rieger, *Science* **1999**, *285*, 2081–2082.
- [25] K. Kageyama, J. I. Tamazawa, T. Aida, *Science* **1999**, *285*, 2113–2115.
- [26] R. Ramachandra Rao, B. M. Weckhuysen, R. A. Schoonheydt, *Chem. Commun.* **1999**, 445–446.
- [27] M. Weckhuysen, R. Ramachandra Rao, J. Pelgrims, R. A. Schoonheydt, P. Bodart, G. Debras, O. Collart, P. Van Der Voort, E. F. Vansant, *Chem. Eur. J.* **2000**, *6*, 2960–2970.
- [28] A. Gräser, S. Spange, *Chem. Mater.* **1998**, *10*, 1814–1819.
- [29] U. Eismann, S. Spange, *Macromolecules* **1997**, *30*, 3439–3446.
- [30] S. Spange, U. Eismann, S. Höhne, E. Langhammer, *Macromol. Symp.* **1997**, *126*, 223–236.
- [31] S. Spange, *Prog. Polym. Sci.* **2000**, *25*, 781–849.
- [32] S. Spange, A. Gräser, P. Rehak, C. Jäger, M. Schulze, *Macromol. Rap. Commun.* **2000**, *21*, 146–150.
- [33] S. Schneider, H. Mayr, P. H. Plesch, *Ber. Bunsenges. Phys. Chem.* **1987**, *91*, 1369.
- [34] H. Mayr in *Cationic Polymerization: Mechanisms, Synthesis, and Applications*, (Ed.: K. Matyjaszewski), Marcel Dekker, New York, **1996**, pp. 51–136.
- [35] S. Spange, Y. Zimmermann, A. Gräser, *Chem. Mater.* **1999**, *11*, 3245–3250.
- [36] C.-Y. Chen, H. X. Li, M. E. Davis, *Microporous Mater.* **1993**, *2*, 17–26.
- [37] R. Guidotti, E. Herzog, F. Bangerter, W. R. Caseri and U. W. Suter, *J. Colloid Interface Sci.* **1997**, *191*, 209–215.
- [38] In the MAS-CP-¹³C {¹H} solid-state NMR spectrum of the product of the reaction between CH₃CH(OC₂H₅)₂ with MCM-41, two signals at $\delta = 58.2$ and $\tau = 58.6$ can be clearly recognised. These can be attributed to both the expected Si-O-C and/or the ether bonds; a) S. Spange, A. Gräser, Y. Zimmermann, P. Rehak, C. Jäger, H. Fuess, C. Baecht, *Chem. Mater.* **2001**, submitted.
- [39] H. Vogel, *Phys. Zeit.* **1921**, *22*, 645.
- [40] G. S. Fulcher, *J. Am. Chem. Soc.* **1925**, *8*, 339–359.
- [41] G. Tammann, G. Hesse, *Z. Anorg. Allg. Chem.* **1926**, *156*, 245–257.
- [42] M. Arndt, R. Stannarius, H. Groothues, E. Hempel, F. Kremer, *Phys. Rev. Lett.* **1997**, *79*, 2077–2080.
- [43] A. Huwe, F. Kremer, P. Behrens, W. Schwieger, *Phys. Rev. Lett.* **1999**, *82*, 2338–2341.
- [44] F. Kremer, A. Huwe, M. Arndt, P. Behrens, W. Schwieger, *J. Phys.: Condens. Matter* **1999**, *11*, A175–A188.
- [45] G. Adam, J. H. Gibbs, *J. Chem. Phys.* **1965**, *43*, 139–146.
- [46] E. Donth, *J. Non-Cryst. Solids* **1982**, *53*, 325–330.
- [47] E. Donth, *Glasübergang*, Akademie Verlag, Berlin **1981**.
- [48] S. Havriliak, S. Negami, *J. Polym. Sci. Part C* **1966**, *14*, 99–117.

Received: January 11, 2001 [F2997]